CNRS
Centre National de la Recherche Scientifique

INFN
Istituto Nazionale di Fisica Nucleare

EGO EUROPEAN GRAVITATIONAL OBSERVATORY

Determination of back scattering and direct reflection recoupling from single optics - application to the End Benches

VIR-0375A-10

B. Canuel, E. Genin

Issue: 1

Date: June 15, 2010

Contents

1 Introduction **2**

2 End benches coupling factor **3**

3 Calculation of relative back scattering P/P_i **4**
3.1 Calculation of P/P_i . . . 4
3.2 Model of diffused light . . . 5
3.3 Calculation of the recoupling function $F(r, \theta, \phi)$. . . . 6
3.3.1 Calculation of the propagation Matrices . . . 6

4 Case of the Virgo End Benches **7**
4.1 Example of calculation for the D1 photodiode . . . 8
4.2 G factor of the different end bench optics . . . 8

5 Understanding the parameters influencing the recoupling **10**

6 Cross-checking of the results with ZEMAX software **11**
6.1 Principle of the computation . . . 11
6.2 Results . . . 12

7 Diffusion vs reflection **14**
7.1 Calculation of recombination on the cavity's eigenmode . . . 14
7.1.1 G in the case of perfectly aligned optics (β=0) . . . 16
7.1.2 G in the real case (β close to 0) . . . 16
7.2 Calculation of G from reflection of L1 . . . 18

8 Conclusion **18**

1 Introduction

Noise hunting on Virgo showed that diffused light of optics placed on the external benches could spoil the ITF sensitivity. This is due to the fact that seismic noise of the optical bench creates some direct and up-converted noise measurable on the dark fringe through the phase-modulation of diffused light re-introduced into the interferometer [1], [2].

In order to help the mitigation of this noise, some studies were realized in the EGO optics lab to identify through the most common Virgo optical components, which were the most diffusing ones [3]. This study was the base for recent diffused light mitigation, carried out by injecting some seismic lines with a shaker placed on the benches. The extra seismic noise was therefore creating some direct and up-converted noise measurable on the dark fringe.

The level of diffused light recoupling, named G, is obtained by the ratio between the measured effect on h and the phase modulation introduced by seismic noise $\phi(t)$ on the considered bench (which can be measured with an episensor seismometer).

$$h = G \sin(\phi(t)) \tag{1}$$

This factor G is therefore measuring the diffused light recoupling of a **complete external bench**. The determination of this factor was useful during Virgo commissioning to assess progresses done during campaigns of diffused light mitigation and compare the results obtained on different benches. It is also very useful to determine the limitation introduced by diffused light on sensitivity by projecting quiet seismic noise present on each bench using equation 1.

The actual value of G measured on each bench after mitigation together with projections on dark fringe noise for Virgo, V+ and AdV can be found in [4].

The aim of this document is to determine the recoupling G of **each of the single optics** composing the external benches starting from laboratory measurement of their diffusion. The quadratic sum of these single recoupling factors should corresponds to the one measured with seismic noise injections. This study is important to understand the parameters influencing the recoupling mechanism. It can also help to determine the biggest contribution to the recoupling among the various benches' optics in order to foresee further improvements.

In order to calculate the recoupling G of scattered light of a single optic we first have to calculate the amount of power P emitted by diffused light that can recouple to the fundamental mode of the Virgo FP cavities. More precisely, we have to calculate the relative quantity $\sqrt{P/P_i}$ where P_i is the incoming power on the external bench considered. As we will see, this quantity $\sqrt{P/P_i}$ depends on the diffusion of the considered optic and on the optical setup placed before this optic. Then this quantity must be multiplied by the optical gain K_{bench} of the FP cavity which will depend on the position of the external bench considered with respect to the FP cavities. Indeed, a perfectly matched beam will not have the same optical gain if injected from the IM or EM side.

$$G = K_{bench}\sqrt{P/P_i} \tag{2}$$

The document will be focused on the situation of the End benches and more particularly on the North End Bench. Indeed, since the change of the NE mirror in June 2008, the situation is quite different on the two terminal benches. Thanks to the addition of an AR coating on the back face of the new NE mirror, it was possible to get rid of many spurious reflections superimposed close to the main beam which are still present on the WEB. For this reason, it is likely that the G value measured on the WEB may be limited by some clipping/dumping of these beams on non proper surface, which is difficult to estimate correctly.

In the first part of this document, we will present the calculation of the K factor for the end benches. Then we will see how to calculate the quantity $\sqrt{P/P_i}$ and give the results of recoupling G for all the optics of these benches and check that the quadratic sum of these recoupling corresponds to the G factor measured by seismic

injection on the NEB. We will then study how the design of the bench influences the recoupling G, which could give a few hints for future external benches design. To finish we will make a further check of this work, by comparing with G calculation done with the Zemax optical design software.

In the second part, we will study a second coupling path of the seismic noise of the external benches that could come from the recoupling of the **specular reflection** of the benches' optics. We will compare the associated G with the one obtained with diffused light.

2 End benches coupling factor

Hereafter is described the way we have estimated the coupling factor of the back-scattered light coming from Virgo end benches in the interferometer (ITF). The coupling factor from end benches presented in previous documents (see [4]) is only approximative. In order to be able to better estimate the recoupling of the back scattered light from end benches in the interferometer, we will clarify this calculation.

It is important to understand that Virgo 3km-long Fabry-Perot cavities are under coupled in the case the light is entering the Fabry-Perot cavities of Virgo from the end mirror. Actually as explained in [5], the gain of a Fabry-Perot cavity is:

$$G_{FP} = \frac{(1+\xi)F}{\pi} \tag{3}$$

where $\xi = \frac{-r_1+r_2(1-p_1)}{1-r_1 r_2}$, r_1 and r_2, respectively, the reflectivity in amplitude of the first mirror and the second mirror of the cavity (depending on the side the light is entering in the cavity) and p_1, the losses of the first mirror that we can consider equal to zero. Considering Virgo input and output mirrors reflectivity, one can find that:

$$G_{FPin} = \frac{2F}{\pi}$$

if you enter from the input mirror and

$$G_{FPend} = \frac{1.56.10^{-4}F}{\pi}$$

if you enter from the end mirror (F is the 3km long Fabry-Perot cavity finesse).

Moreover, Virgo interferometer is a bit more complex than a simple Fabry-Perot cavity since there is a power recycling cavity that allows to enhance the sensitivity of the gravitational wave detector at high frequency (above a few hundred of Hz). A simplified scheme of this double cavity configuration is given on figure 1. In order to estimate the gain of the Fabry-Perot cavity in this case, one should consider a cavity made by the FP cavity end mirror and the power recycling cavity. The effective reflectivity of the power recycling cavity at resonance is:

$$R_{effPR} = \left(\frac{-\sqrt{R_{PR}}+\sqrt{R_{in}}}{1-\sqrt{R_{PR}R_{in}}}\right)^2$$

with R_{PR}=0.95, R_{in}=0.88 and R_{end}=0.99999 (Virgo configuration). In this case the effective reflectivity of the PR cavity is 0.18248. In the same way, we can calculate the effective reflectivity of the cavity formed by the PR cavity and the end mirror and we find ξ=-0.9999875426. In this configuration, the gain of the cavity becomes $G_{FPend} = \frac{1.2457.10^{-5}F}{\pi}$. This result has been cross-checked with Finesse simulation of the double cavity.

Thus, the power of the field back-scattered by a diffusing element on the end benches which is recoupled in the interferometer is:

$$P_{sc} = P_{cav}T_{end}f_{sc}\frac{1.2457.10^{-5}F}{\pi}$$

Following the explanation given in [6], we can write the coupling factor K_{end} as:

$$K_{end} = \frac{\lambda}{8L}\sqrt{\frac{T_{end}.1.2457.10^{-5}}{\pi F}}$$

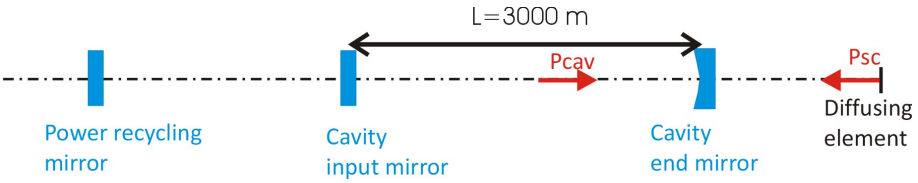

Figure 1: Double cavity configuration of the Virgo interferometer.

With L= 3000 m; T_{end}=10^{-5} and F=50, we find K_{end}=$3.948.10^{-17}$.

Comparison of K_{end} value for Virgo, Virgo+ with the former and the new method of back-scattered light coupling estimation is given in table 1.

Interferometer	T_{end}	F	R_{PR}	R_{in}	$K_{end-old}$	$K_{end-new}$
Virgo	10 ppm	50	0.95	0.88	5.10^{-17}	$3.95.10^{-17}$
Virgo+ with MS	3.7 ppm	150	0.95	0.959	$1.07.10^{-17}$	$5.3.10^{-18}$

Table 1: K_{end} estimation with old formula [6] ($K_{end-old}$) and the refined formula ($K_{end-new}$).

3 Calculation of relative back scattering P/P_i

In this section we will study how to calculate the relative back scattering P/P_i from an optical surface placed on an external bench. These calculations will be done using the supposition that the diffusing surfaces are Lambertian. This is a reasonable supposition done for many diffusing surfaces which means that their BRDF is constant [7]. Such surfaces can be characterized by their total relative integrated scattering value α that we could measure in the EGO optics Lab. Using a model of recombination to the main beam for photons emitted from these surfaces, we will see that these measurements enable to calculate the quantity P/P_i.

3.1 Calculation of P/P_i

A single photon emitted from the diffusing surface can be described by its emitting position

$$M : \begin{pmatrix} x \\ y \\ 0 \end{pmatrix}$$

(the origin along z optical axis is taken at the emitting source) and its normalized direction

$$\overrightarrow{d} = \begin{pmatrix} u \\ v \\ w \end{pmatrix}$$

In fact the recoupling problem gets a cylindrical symmetry and we can limit the calculation to small polar angles (paraxial like approximation). The relevant parameters will then be the distance from optical axis r and the normalized direction vector

$$\begin{pmatrix} \phi\cos(\theta) \\ \phi\sin(\theta) \\ 1 \end{pmatrix}$$

(see figure 2). For a photon described by these parameters, we define the boolean recoupling function $F(r, \theta, \phi)$ which is equal to 1 if the photon is recoupled, 0 otherwise. The relative power recoupled by a diffusing surface covering the whole beam of intensity I(r) can be written:

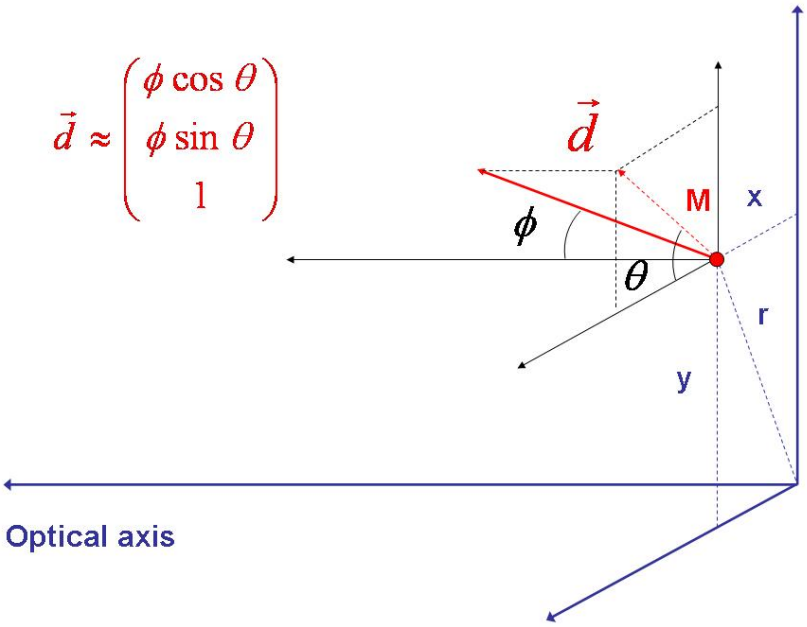

Figure 2: A single photon can be described by its emitting point M and normalized direction d

$$P/P_i = \frac{1}{P_i}\int_0^{\infty}\int_0^{2\pi} rI(r)d^2P(r)d\alpha dr$$

where

$$d^2P(r) = \int_0^{2\pi}\int_0^{\pi/2}\frac{dP}{d\Omega}\sin(\phi)F(r,\theta,\phi)d\theta d\phi$$

3.2 Model of diffused light

We make the common assumption that the considered optical surfaces are Lambertian. This means that the BRDF (scattered radiance) of the surface is constant. In other words, for a incident power P_i on the surface:

$$\frac{dP}{d\Omega} = KP_i\cos(\phi)$$

To determine the parameter K, we measure the diffused light power P_0 at a distance R from the surface. The detector is placed normally with respect to the sample ($\phi = 0$).

Around $\phi = 0$ we have $K = \frac{1}{P_i}\frac{dP}{d\Omega}$ with $P_i = 700$ mW is the incident power. In this measurement, we then have: $d\Omega = 4\pi\frac{A_d}{4\pi R^2}$ where A_d =1 cm^2 is the surface of the detector and $dP = P_0$.

Therefore:

$$K = \frac{P_0R^2}{P_iA_d}$$

The total relative integrated scattering α of the optical surface is related to K:

$$\alpha = \frac{1}{P_i}\int_0^{2\pi}\int_0^{\pi/2}\frac{dP}{d\Omega}\sin(\phi)d\theta d\phi$$

$$\alpha = \pi K$$

Table 3 summarizes measured α values for various optics of the end benches.

Using this model, we can then write:

$$P/P_i = 2\alpha \int_0^{\infty} \int_0^{2\pi} \int_0^{\pi/2} rI(r)\cos(\phi)\sin(\phi)F(r,\theta,\phi)drd\theta d\phi$$

3.3 Calculation of the recoupling function $F(r,\theta,\phi)$.

In this section we explain how to calculate $F(r,\theta,\phi)$. To do this, we realize the propagation of the photon inside the optical system placed on the external bench. Then the photon is propagated trough one of the virgo cavities. The photon is considerated resonant if it couples through both systems. It means that it should not superate the different optical apertures. In the case of the cavity propagation, the photons should make a number of round trips equal to the finesse $F/2\pi$ without getting out of the mirror coatings. Therefore, for a given photon emitted by the scattering surface (that we suppose here placed perpendicularly to the beam propagation, which is the worst case), we calculate its coordinates x_i, y_i, z_i in the plane of the optical component number i and check if $(x_i^2 + y_i^2)^{\frac{1}{2}} < a_i$ were a_i is the radius of this component.

3.3.1 Calculation of the propagation Matrices

As we said before, a single photon at any instant of its propagation can be described by the vector

$$\begin{pmatrix} x \\ y \\ z \\ \phi\cos(\theta) \\ \phi\sin(\theta) \\ 1 \end{pmatrix}$$

It can be easily shown that the propagation matrix on a free distance d, named $P(d)$, can be written:

$$P(d) = \begin{pmatrix} 1 & 0 & 0 & d & 0 & 0 \\ 0 & 1 & 0 & 0 & d & 0 \\ 0 & 0 & 1 & 0 & 0 & d \\ 0 & 0 & 0 & 1 & 0 & 0 \\ 0 & 0 & 0 & 0 & 1 & 0 \\ 0 & 0 & 0 & 0 & 0 & 1 \end{pmatrix}$$

In order to calculate the propagation matrix trough a thin lens of focal f, named $L(f)$, it is possible to extend the planar geometrical construction: the image beam crosses the intersection point between the focal plane and the beam parallel to the object beam passing through the center of the lens. Then it comes:

$$L(f) = \begin{pmatrix} 1 & 0 & 0 & 0 & 0 & 0 \\ 0 & 1 & 0 & 0 & 0 & 0 \\ 0 & 0 & 1 & 0 & 0 & 0 \\ -\frac{1}{f} & 0 & 0 & 1 & 0 & 0 \\ 0 & -\frac{1}{f} & 0 & 0 & 1 & 0 \\ 0 & 0 & 0 & 0 & 0 & 1 \end{pmatrix}$$

The optical system may be described as a succession of elementary matrixes M_i of type L or P. These matrices enable a fast calculation of the full propagation matrix R_i on the element i. $R_i = \prod_{j=1}^{i} M_i = M_i P_{i-1}$ then

$$F(r,\theta,\phi) = (\parallel R_1.u(r,\theta,\phi) \parallel < a_1) \wedge (\parallel R_2.u(r,\theta,\phi) \parallel < a_2) \ldots \wedge (\parallel R_k.u(r,\theta,\phi) \parallel < a_k)$$

where a_i is the optical aperture of element i and where the norm corresponds to the distance of the photon from the optical axis:

$$\parallel \begin{pmatrix} x \\ y \\ z \\ \phi\cos(\theta) \\ \phi\sin(\theta) \\ 1 \end{pmatrix} \parallel = (x_i^2 + y_i^2)^{\frac{1}{2}}$$

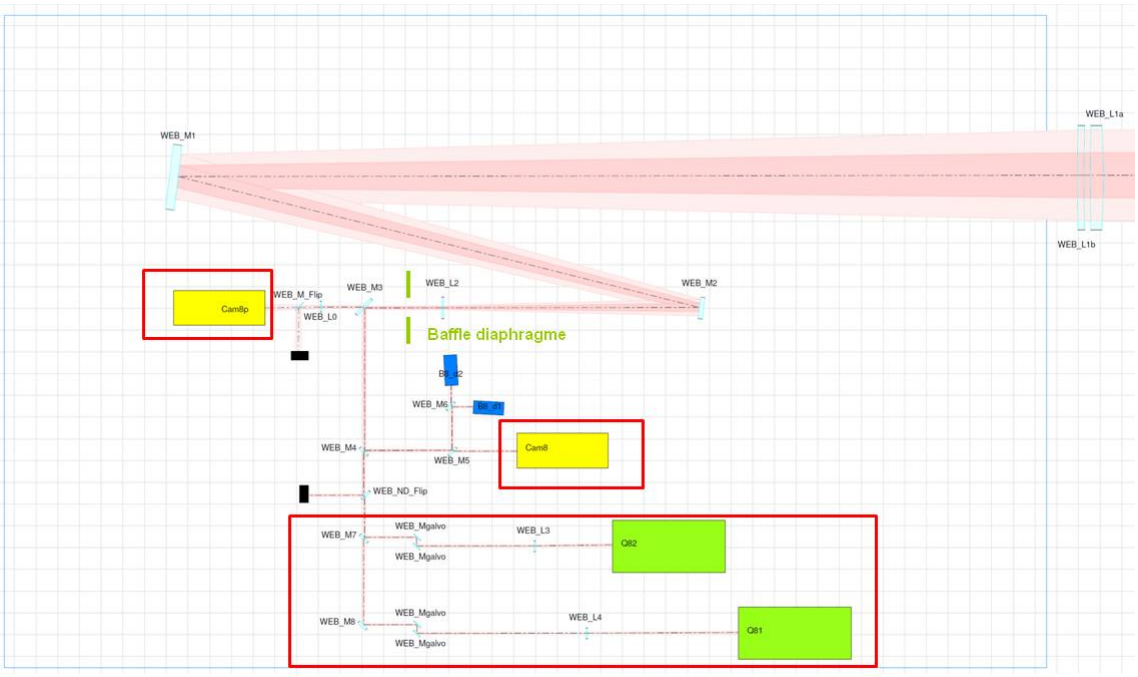

Figure 3: Optical layout of the Virgo end benches. On the parts circled in red, the impinging power is less than a 1% of incoming power on the bench. These elements will then have a negligible contribution to the total back scattering of the whole setup.

4 Case of the Virgo End Benches

In this section we will use the method previously explained to calculate the recoupling of different single optical elements of the Virgo End benches. We will validate these calculations by cross checking with the G measurement that corresponds to the sum of all the contributions of these single elements.

These calculations will enable to identify the most critical elements and deduce the possible improvements.

The optical setup of the Virgo End bench can be seen on figure 3. On this setup, most of the power is located inside the telescope L1-L2 and the path to the photodiodes D1-D2. For this reason, we will not consider the parts of the bench circled in red in figure 3.

4.1 Example of calculation for the D1 photodiode

In this section, we give an example of calculation for the D1 photodiode. The propagation matrixes R_i are given in table 2 together with the optical apertures of the corresponding i-th optic.

R_i	Propagation on:	Aperture a_i (cm)
$R_1 = P(0.05)$	M6	1.25
$R_2 = P(0.1).R_1$	M5	1.25
$R_3 = P(0.2).R_2$	M4	1.25
$R_4 = P(0.328).R_3$	M3	2.25
$R_5 = P(0.09).R_4$	Baffle Diaphragm	0.75
$R_6 = P(0.09).R_5$	L2	2.5
$R_7 = P(0.5897).L(-229.5).R_6$	M2	2.5
$R_8 = P(1.237).R_7$	M1	7.5
$R_9 = P(2.096).R_8$	L1	11.2
$R_{10} = P(3).L(4.1144).R_9$	Back face of End mirror	17.5
$R_{11} = P(3000).L(2 * 3500).R_{10}$	Input mirror coating	10
$R_{12} = P(3000).R_{11}$	End mirror coating	16.5
... for n= 1...49		
$R_{2n+11} = .P(3000).L(3500).P(3000).R_{2(n-1)+11}$	Input mirror coating	10
$R_{2n+12} = P(6000).L(3500).R_{2(n-1)+12}$	End mirror coating	16.5

Table 2: Calculation of the propagation matrixes R_i for a photon emitted from D1

Then we obtain the function F as explained before:

$$F(r,\theta,\phi) = \parallel R_1.u(r,\theta,\phi) \parallel < a_1 \wedge \parallel R_2.u(r,\theta,\phi) \parallel < a_2 \ldots \wedge \parallel R_k.u(r,\theta,\phi) \parallel < a_k$$

In order to calculate G, we have to take into account the actual impinging power on D1: With r_{M3},r_{M4},r_{M5} and t_{M6} the reflection and transmission of M3,M4,M5 and M6: (the other element are considered perfectly reflective or transmissive).

$$P/P_i = (r_{M3}r_{M4}r_{M5}t_{M6})^2 2\alpha_{D1} \int_0^\infty \int_0^{2\pi} \int_0^{\pi/2} rI(r)\cos(\phi)\sin(\phi)F(r,\theta,\phi)drd\theta d\phi$$

Where α_{D1} the relative total diffused light emitted from D1. $I(r)$ is the Intensity on D1, calculated propagating a gaussian beam in the optical setup before this element, starting with a waist of 2.15 cm located on the input mirror.

Then:

$$G_{D1} = \frac{\lambda}{8L}\sqrt{\frac{T_{end}.1.2457.10^{-5}}{\pi F}}\sqrt{P/P_i}$$

and we obtain:

$$G_{D1} = 0.8 \times 10^{-21}$$

4.2 G factor of the different end bench optics

In table 3 we give the characteristics of all the elements considered and the measure of their relative total diffused light $\alpha = \pi K$. We can then calculate their associated G factor using the method explained in section 4.1.

Name	Type	Manufacturer	α(ppm)
L1	Doublet f=4,1144m	Silo	100
M1,M2	HR mirrors	Silo	75
L2	Lens f=-229.5mm	CVI	20
BeamDump2	Razor blades	Thorlabs	5000
M_Flip	R=99% mirror	Fichou	200
M3,M4,M5	R=90%,R=50%,R=99%	CVI	500
L0	Lens f=-50mm	CVI	20
BeamDump1	Absorbing glass	Shott	15
ND_flip	Neutral density	CVI	20
M6	R=10%	Fichou	85
d1, d2	Photodiodes	Hamamatsu	1250

Table 3: Parameters used for G calculation

These results are summarized in figure 4 where we can observe that the main contribution comes from the D1 photodiode with a G close to 10^{-21}. Then come the M3 M4 and M5 mirrors which recouples quite a lot (a few to 10^{-22}) due to their high scattering.

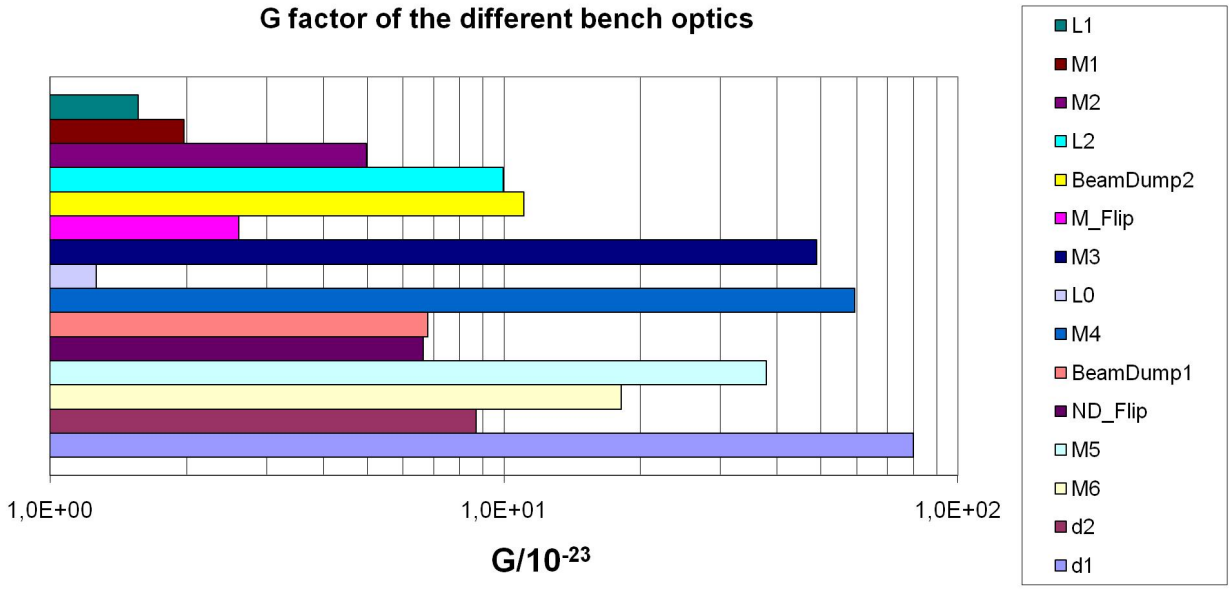

Figure 4: Calculated G for main optics of the end bench

The quadratic sum of all the elements corresponds to: $G_{tot} = 1.2 \times 10^{-21}$ which is very close to the value measured for the whole bench by noise injection [8] $G_{measured} = 1.4 - 1.8 \times 10^{-21}$.

We can observe that most of the contribution to G_{tot} comes from optics after L2. All contribution of optics inside the L1-L2 telescope are about one order of magnitude smaller than G_{tot} (the biggest contribution inside the telescope being L2 itself with $G_{L2} = 1 \times 10^{-22}$).

Of course, this can be explained because the most diffusing optics (D1,M3,M4 and M5) are placed after L2. But this is especially due to the fact that the recoupling is intrinsically much more efficient after L2 than between L1-L2 as we will see hereafter.

5 Understanding the parameters influencing the recoupling

As calculated with previous method, the recoupling both depends on the value of the waist of the incoming beam (ω_0) and the position of the diffusing element with respect to this waist.

To illustrate this fact, we study here the situation after L1 (and will forget here about the other optics on the bench). For a focal of f=4.11 m (actual value), the waist size obtained is ω_0=26.8 μm located at 4.12 m from L1. Figure 5 plots the recoupling G of a diffusing element ($\alpha = 1$) placed at a variable distance from this lens. We observe that G is maximum when the object gets close to the waist position. This can be easily explained by the fact that when the source of diffused light gets close to the waist of the incoming beam (which is in this case very close to the focal point of the lens), all the light diffused inside the solid angle $\pi\frac{a^2}{f^2}$ (where a and f are respectively the aperture and the focal of the lens) goes back collimated inside the cavity after passing back through L1, and has therefore a good chance to resonate inside the cavity.

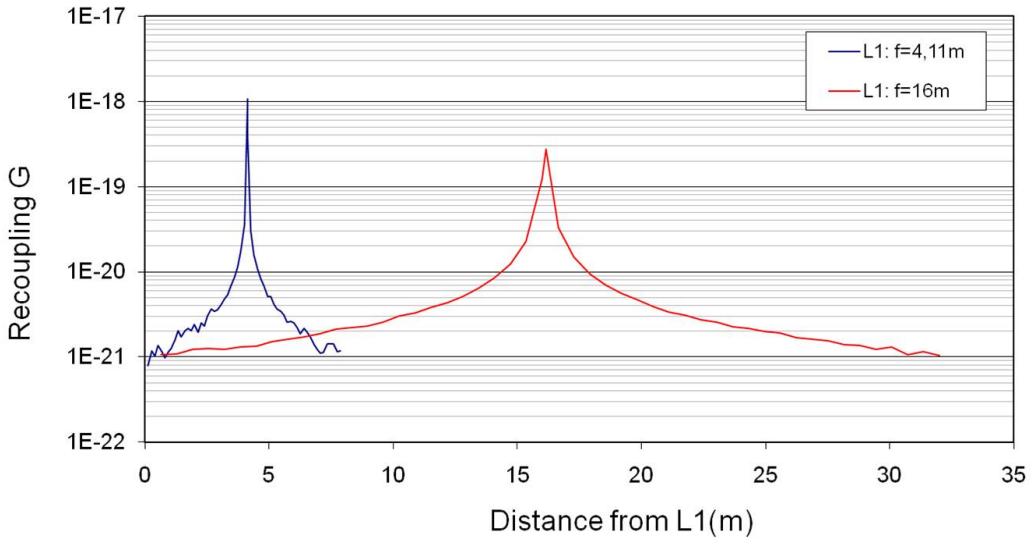

Figure 5: G factor for an optic of α=1 placed after L1 (with no other optic on the bench) for a focal of L1 of 4.11 m (actual value) and 16 m.

In order to see how G scales with the waist value, we can also plot the same curve with different values of focal. For a focal of f=16 m, the waist size is ω_0=105 μm and located at about 16.14 m from the lens. We observe on figure 5, that in this case the recoupling changes more slowly around the waist location and that the maximum value of recoupling is lower than with $f \approx$4 m.

From these plots, it seems reasonable to consider that to lower the back recoupling on the external benches, waist size should be as big as possible and optics should be placed as far as possible from the waist location. Of course, we considered here the particular case of recoupling just behind the FP cavities and a complete discussion should take into account all optics placed before the diffusing element considered.

To finish, we study the real case of the L1-L2 telescope. Figure 6 plots the recoupling G as a function of distance from L1, for an optical element of α=1 placed somewhere inside (0<distance<3.9 m) or after (distance>3.9 m) the telescope. We observe that the recoupling is much more important if the object is placed after the telescope (distance>3.9 m). This could seem a contradiction with the previous consideration because the waist of the beam inside the telescope (ω_0=26.8 μm) is much smaller than after the telescope (ω_0=200 μm). But in fact an element placed inside the telescope (where the waist is virtual after L2) is always far from the location of the waist. This is no more true after L2 where the waist is located at 1.17 m after this lens.

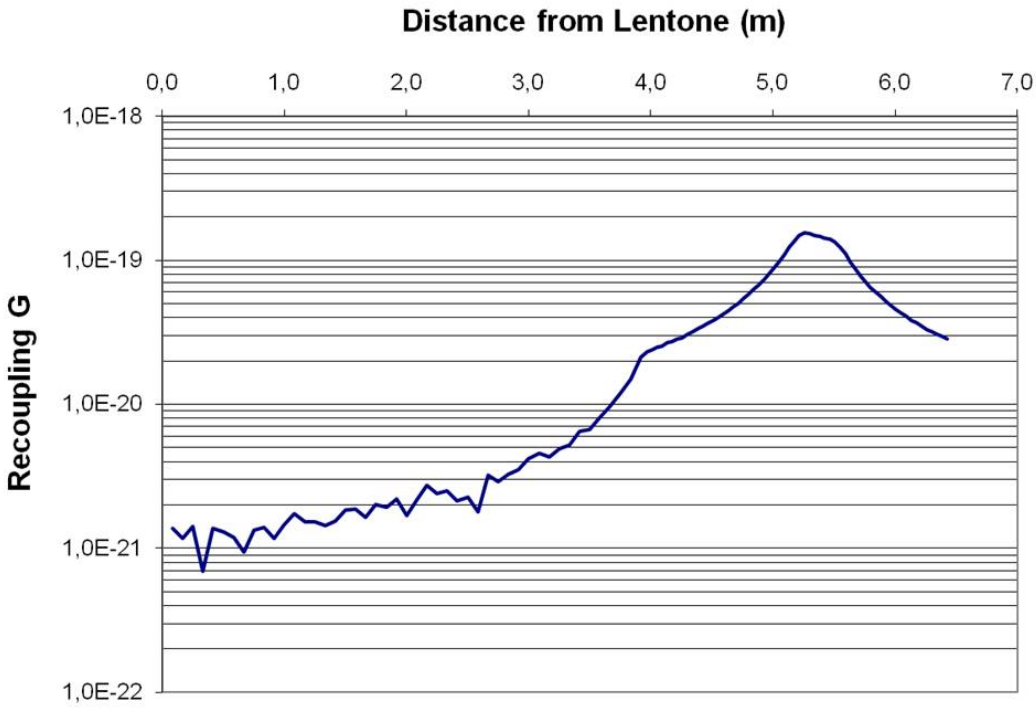

Figure 6: G factor for an optic of α=1 placed inside or outside the L1-L2 telescope as a function of its distance from L1.

6 Cross-checking of the results with ZEMAX software

In this section, we will present results obtained with a computation done with Zemax optical software that has been made to cross-check the results obtained by the model presented in the previous sections.

6.1 Principle of the computation

There is the possibility with Zemax software to compute the quantity of light scattered by an optical element that impinges on a defined target. There are 2 methods that can be used in Zemax to model scattering efficiently we choose Important sampling (see Zemax Manual). The principle of this method is to always scatter the ray towards the object of interest, and then to normalize the energy the ray carries to account for the probability the ray would have actually scattered in that direction. This method is very efficient if the scatter is narrow angle or the object of interest subtends a relatively small angle as seen from the scattering surface which is the case for our study. We have to define the Total Integrated Scatter (TIS) that is corresponding to the integral of the Bi-Directional Scatter Distribution Function (BSDF) over all possible scatter angles (a hemisphere). The TIS indicates the total fraction of energy that scatters. All remaining energy is assumed to be specular. For our study we considered that the BSDF is Lambertian as done in the previous sections of the document and that the diffusing object is only diffusing (no specular reflection) since in most cases a very small tilt of the diffusing optical element is enough to not re-couple the direct reflection in the Fabry-Perot cavity (see section 7). In order to simulate a cavity, we had to decompose also the cavity as a succession of elementary cells that consist of the FP cavity curved end mirror and the FP cavity flat mirror distant of 3000 meters as shown on figure 7. The end mirror radius of curvature being about 3500 meters, the equivalent lens has a focal lens of 1750 meters.

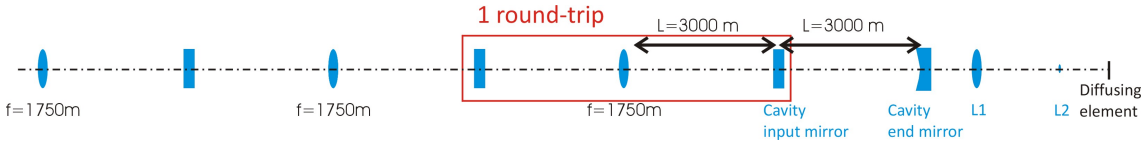

Figure 7: Principle of the modeling of diffusion of an optical element located after L2 lens on the end bench.

Some 3 dimensional views of optical system give a good idea of how is made the computation (see figure 8). As you can see on these pictures, some diaphragms are used to define the finite aperture of the optics of the Fabry-Perot cavity.

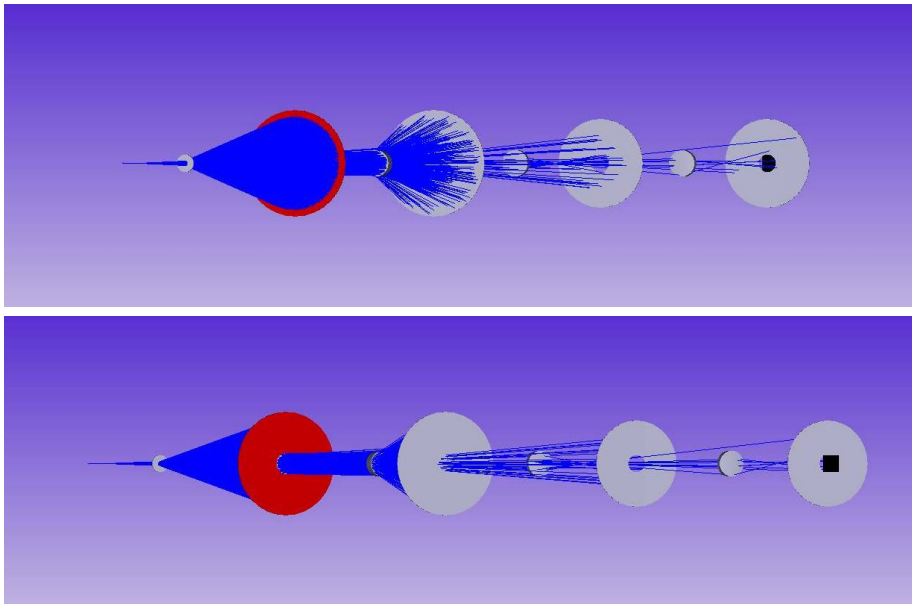

Figure 8: 3D views of the Zemax simulation. The blue rays are the stray light rays generated at the level of the scattering element (white square) that are traveling back to the optical system (End bench telescope and Virgo Fabry-perot cavity). A detector (black square) is recording rays that are hitting the cavity input mirror after a given amount of round-trips (depending on the cavity Finesse).

6.2 Results

On figure 9 you can find a plot of G coupling factor computed with Zemax compared with computation made using the diffused light modeling presented in the previous sections. The two curves agree quite well.

The broader curve obtained by our analytical code is due to the different way we propagate the beam on the diffusing optic. In the analytical code, the laser is propagated using gaussian optics and recombination is calculated with geometrical optics. That's why the curve seems to present two very close maximums. On the contrary, Zemax uses geometrical optics for both calculation.

The back-scattered light intensity profile after 10 round-trips (close to $F/2\pi$) in the Fabry-Perot cavity is given in figure 10.

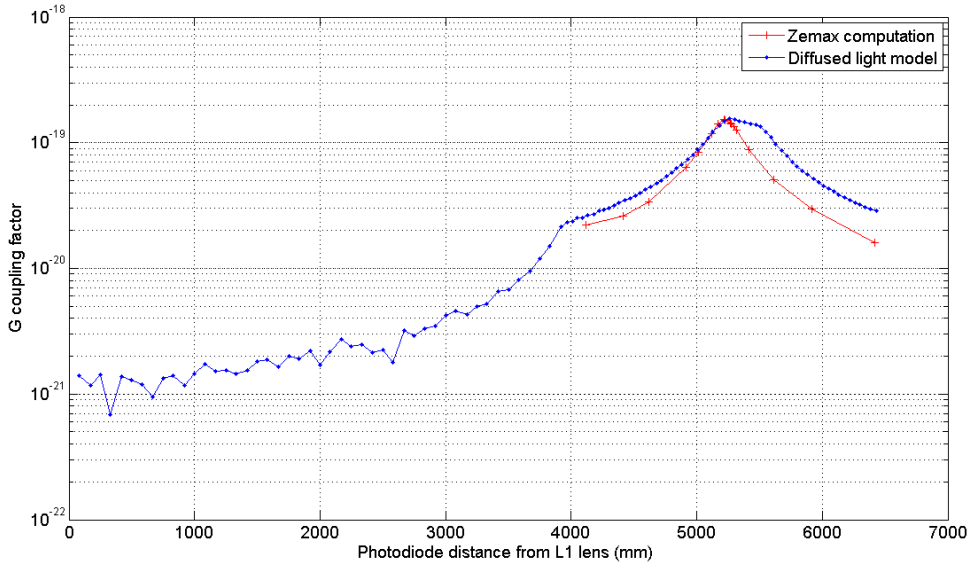

Figure 9: G factor for a diffusing element (10 mm*10 mm) placed after L1 with a lambertian diffusion profile with TIS=1 computed with Zemax (red curve) and Diffused light model (blue curve).

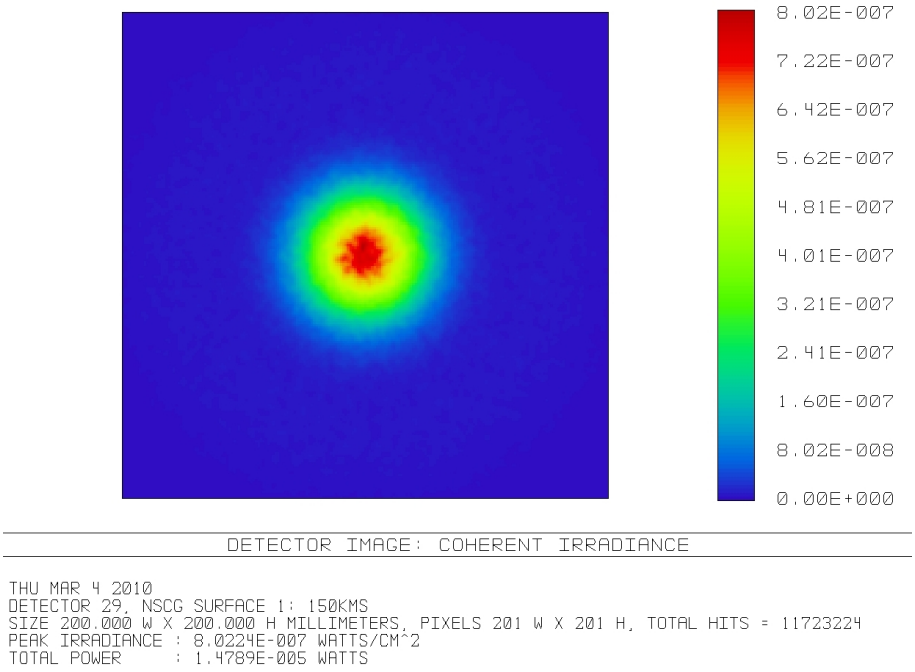

Figure 10: Detector view at Virgo input mirror location after 10 round trips in the Fabry-Perot cavity when the diffusing element is located at the waist of L1 L2 telescope.

7 Diffusion vs reflection

We considered in this note that all contribution to G was coming from diffused light. This may not seem so obvious as some recoupled light could come from simple reflection of the end bench optics.

The reflection on these optics creates a gaussian beam with a beam size ω_1 that can recombine to the fundamental mode of the cavity (waist ω_0 located on the input mirror). After recombination, this light introduces some phase noise by the same mechanism as diffused light. In the following we will see how to calculate this contribution and will examine one example on the NEB: the reflection from the lens L1.

7.1 Calculation of recombination on the cavity's eigenmode

We consider that the reflection on external bench creates a waist ω_1 at a distance L from the input mirror. We also consider that the optic is tilted with an angle β from the optical axis of the cavity.

The amplitude of the TEM_{00} mode on the NI mirror can be written :

$$A_0(x,y) = \sqrt{\frac{2}{\pi\omega_0^2}} \exp\left(-\frac{x^2+y^2}{\omega_0^2}\right)$$

After propagation over a distance z_1, the amplitude of the reflected beam can be written:

$$\begin{aligned} A_1(x_1,y_1) &= \sqrt{\tfrac{2}{\pi\omega_1(z_1)^2}} \exp\left(-\tfrac{x_1^2+y_1^2}{\omega_1(z_1)^2}\right) \exp\left(-\tfrac{\imath\pi}{\lambda R(z_1)}(x_1^2+y_1^2)\right) \exp\left(\imath \arctan\left(\tfrac{z_1}{z_{R1}}\right)\right) \\ &\quad \exp\left(-\imath\tfrac{2\pi}{\lambda}z_1\right) \end{aligned}$$

where:

$$\omega_1(z_1)^2 = \omega_1^2\left(1+\frac{z_1^2}{z_{R1}^2}\right)$$

$$R(z_1) = z_1\left(1+\frac{z_{R1}^2}{z_1^2}\right)$$

$$z_{R1} = \frac{\pi\omega_1^2}{\lambda}$$

The optic being tilted by an angle β, we have at the level of the NI mirror: $x_1 = x$ and $y_1 = y - 2D\beta$ and $z_1 = L + 2\beta y$ (see figure 11), then:

$$\begin{aligned} A_1(x,y) &= \sqrt{\tfrac{2}{\pi\omega_1(L+2\beta y)^2}} \exp\left(-\tfrac{x^2+(y-2D\beta)^2}{\omega_1(L+2\beta y)^2}\right) \exp\left(-\tfrac{\imath\pi}{\lambda R(L+2\beta y)}(x^2+(y-2D\beta)^2)\right) \\ &\quad \exp\left(\imath\arctan\left(\tfrac{L+2\beta y}{z_{R1}}\right)\right) \exp\left(-\imath\tfrac{2\pi}{\lambda}(L+2\beta y)\right) \end{aligned}$$

if R is the reflection of the optic, the relative power recoupled to the main beam is:

$$P = R * |\langle A_0(x,y), A_1(x,y)\rangle|^2$$

And G can be calculated by:

$$G = \frac{\lambda}{8L}\sqrt{\frac{T_{end}.1.2457.10^{-5}}{\pi F}}\sqrt{P}$$

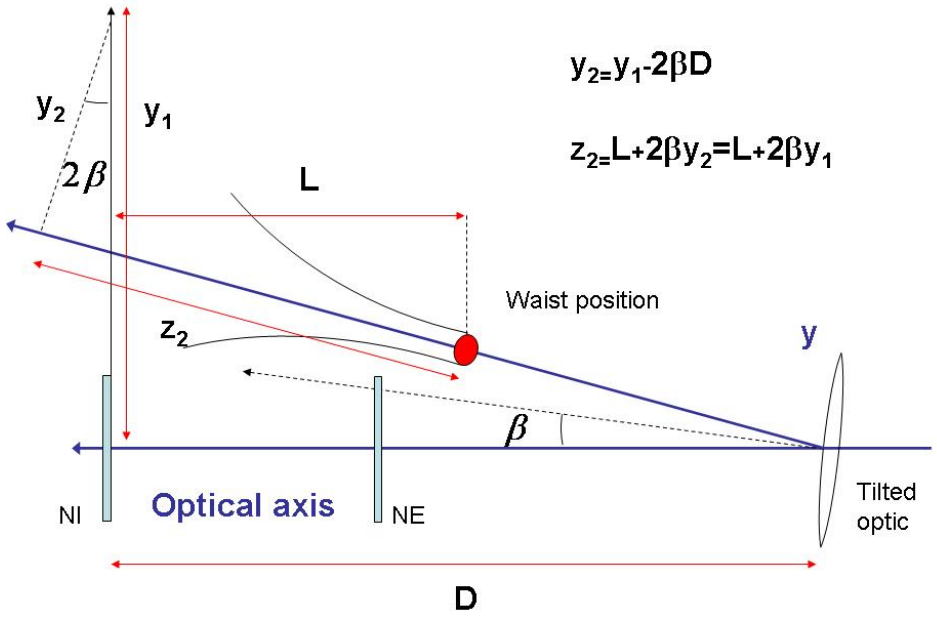

Figure 11: The tilted optic on the external bench creates a beam waist w_1 located at a distance L from the input mirror. The optic itself is placed at D from the NI.

7.1.1 G in the case of perfectly aligned optics (β=0)

We consider here the situation of perfectly aligned optics with a reflection coefficient of 0.5%. On figure 12 we plot the value of Log_{10}(G) respect to L and ω_1. We observe that only very small beam waist (a few microns) or very long distance can lead to G values of less than 10^{-21}. For most situation we then find that recombination by reflection could be a more limiting effect than diffused light ($G = 10^{-21}$ is the maximum value calculated with only diffusion).

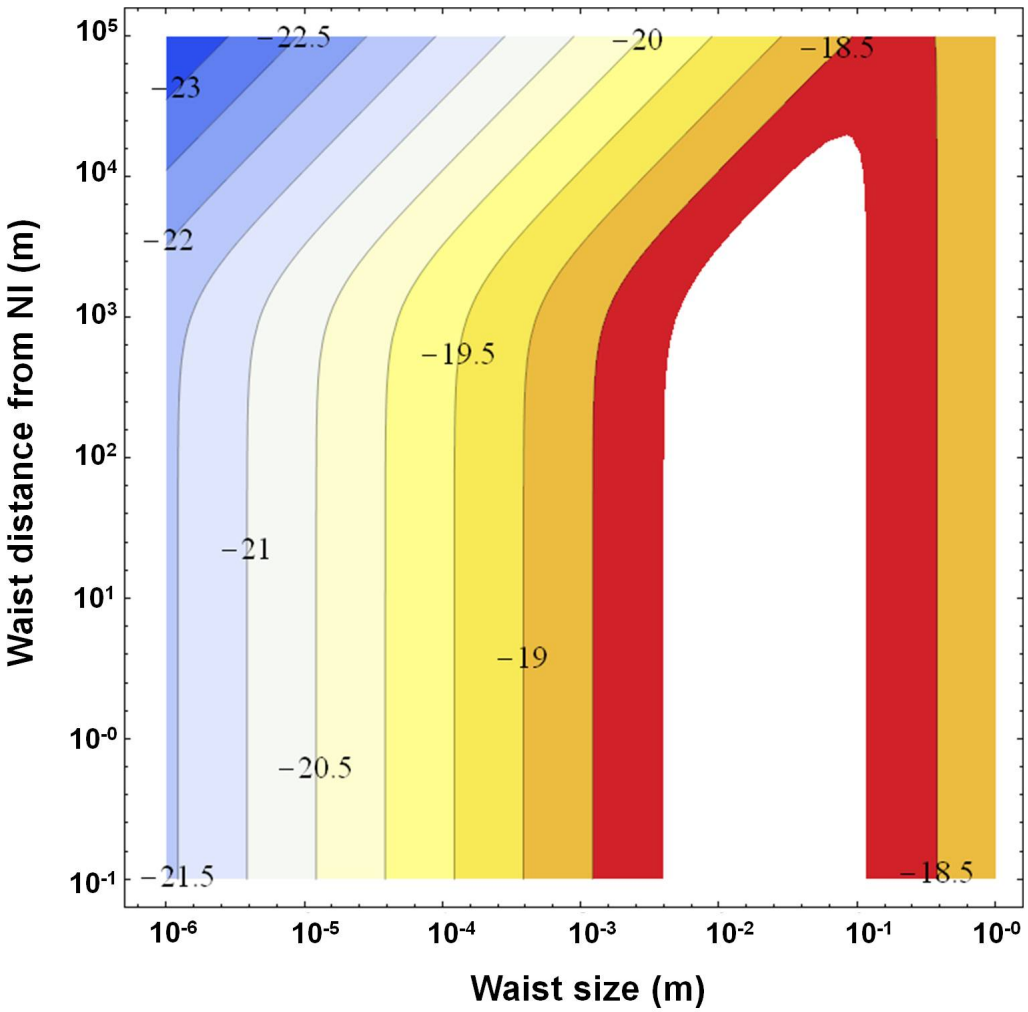

Figure 12: Log_{10}(G) as a function of L and w_1 for the case of a perfectly aligned optic (β=0)

Of course, the supposition that the optics are perfectly aligned is not realistic, and actually all the optics on the bench are voluntary tilted in order to correctly dump their reflection. In the following we study the variation of G as the function of the tilt angle β of the optic considered.

7.1.2 G in the real case (β close to 0)

On figure 13 we consider the case of a reflection (R=0.5%) creating a beam waist of variable size located at different distances from the NI mirror. We observe that when the waist is located far enough from the reflecting element (i.e. far from L=3000m), the recoupling becomes negligible for angles bigger that a few tens of μrad

whatever is the beam size. When the waist is located close to the reflecting element (L≈3000m), the discussion depends on the waist of the beam and recombination can be non negligible for angle as big as a few mrad.

On the NE bench, most of the optics are tilted by a few degrees and therefore their G due to reflection is negligible. Nevertheless it is not the case for the L1 doublet that was voluntarily aligned perpendicularly to the main beam in order to minimize the aberration inside the L1-L2 telescope. The reflection on this element can be a real problem as the curvature of its faces being as small as a few meters, it will create beams with very small waists. Being of a few microns these waists will be therefore located in the vicinity of the bench, which means that we have to consider L≈3000m. As we saw on figure 13 this corresponds to the most critical situation.

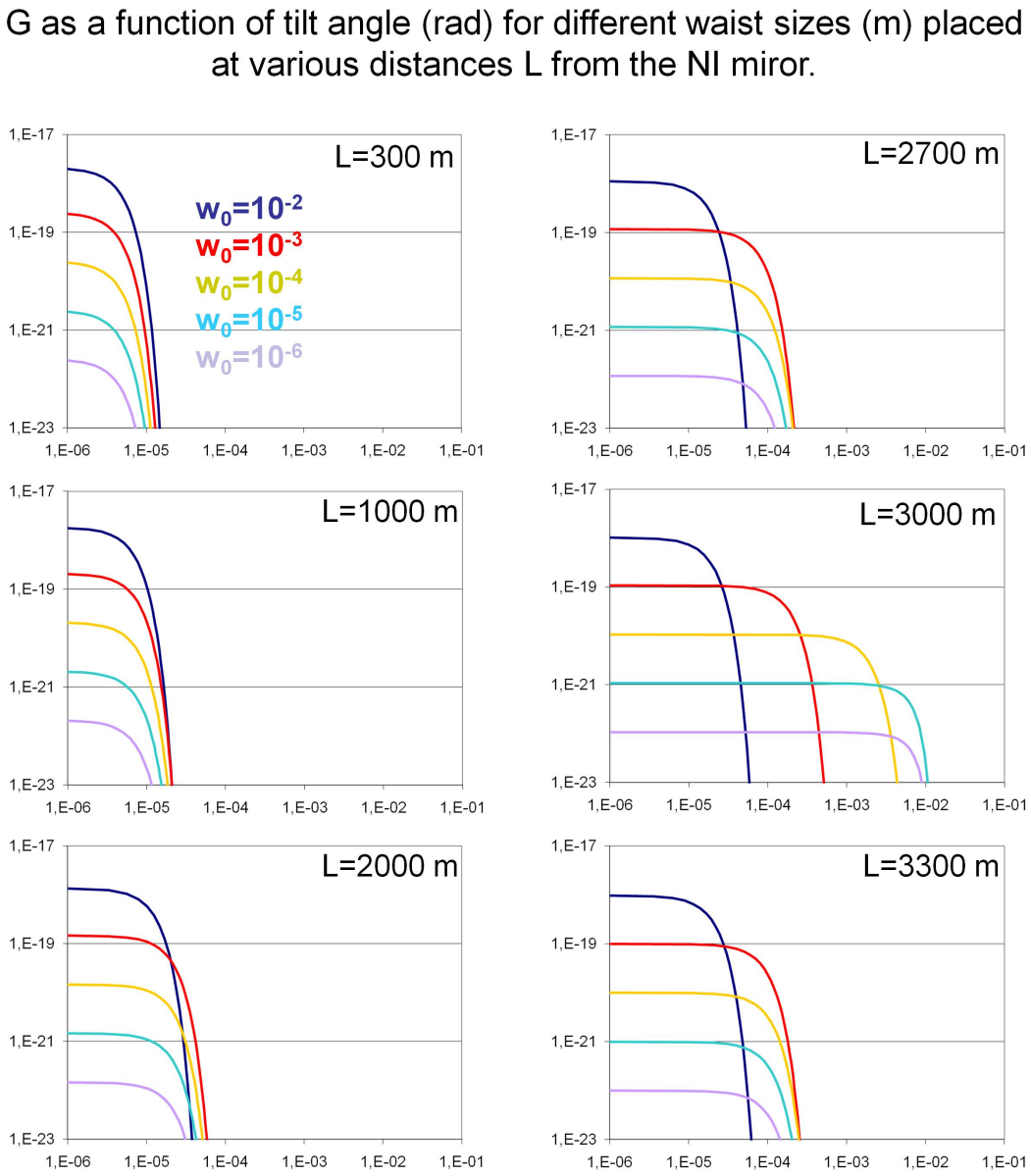

Figure 13: Recoupling G as a function of tilt angle. Calculation is done for various waist sizes and different distances from the NI mirror.

7.2 Calculation of G from reflection of L1

Reflection from the first side of L1 creates a beam waist (after crossing the NE mirror to enter the cavity) of ω_1=7.1 μm located 4.08 m before the NE mirror (i.e.:L=3004 m). Figure 14 plots the recoupling factor of this beam as a function of the tilt of L1. As explained before, as the waist is located around L=3000 m (the most critical situation), we observe an important recoupling (G of 2-3 10^{-21}) for angles up to 20 mrad (about one degree). Reflection coming from other surfaces of the doublet will give similar results (the second lens of the doublet has a focal of f=-17.47 m). As we said before, as this element is placed quite perpendicular to the incident beam, it is therefore not possible to exclude a contribution of **reflection** to the G measured by seismic injection.

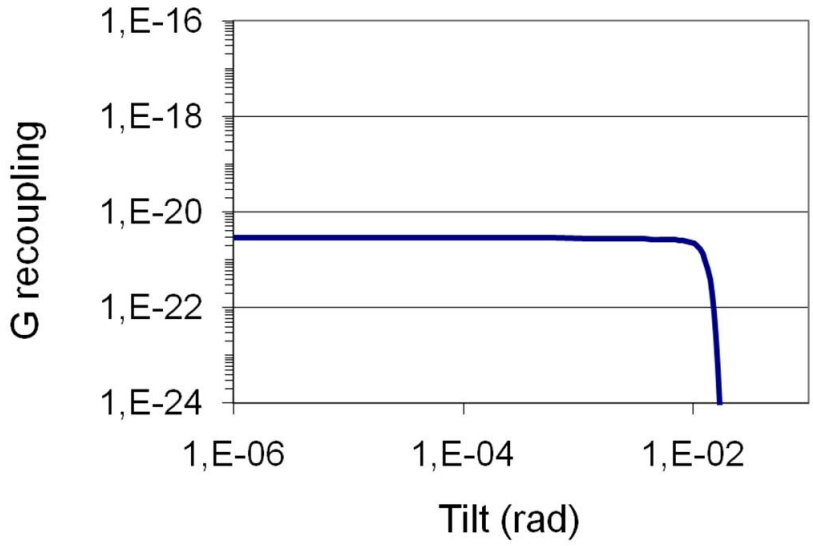

Figure 14: Recoupling G by reflection of the first face of the L1 as a function of its tilt angle

8 Conclusion

In this note, we presented a method to calculate the recoupling factor G by **diffused light** of single elements placed on the external benches. This work could be used in complement of noise hunting carried out with seismic injection to realize further improvements on the bench. We showed that the recoupling factor depends not only, of course, of the diffusion of the optics, but also on the optical setup used on the benches. This opens new possibilities of improvement and could help the design of new external benches for AdV. We used independent measures of diffusion done in the EGO optics lab to calculate the recoupling of all the optics on the actual end benches. We could identify the most limiting element as D1 photodiode. We were able to compare the quadratic sum of all single recoupling G with the one measured with seismic injection on the NEB. We found very close results (1.2 10^{-21} instead of 1.4-1.8 10^{-21}). The difference could be explained by some recoupling by **reflection** as we showed that the L1 lens could recouple up to 2-3 10^{-21} depending on its tilt. The recoupling by reflection of the rest of the bench being negligible as all the other optics are tilted by macroscopic angles. In order to discriminate between **diffused light** and **reflection** recoupling on the NEB, it could be possible by seismic injection to measure the contribution of only L1 by placing a large absorbing glass just behind it.

Calculation parameters

We give in table 4 a few parameters used in calculation of sections 4 and 5.

Parameter	Value
f_{eff}^{L1}	4114.4 mm
f_{eff}^{L1}	-229.5 mm
R_{end}	3500 m
d_{In-End}	3000 m
d_{End-L1}	3 m
d_{L1-L2}	3925.1 mm
FP Cavity waist	21.5 mm

Table 4: Parameters used in calculation of sections 4 and 5

These parameters gives the following beam characteristics on the external bench:

After L1: ω_0=27 μm located at 4124 mm from L1.

After L2: ω_0=200 μm located at 1479 mm from L2.

References

[1] S. Braccini, *Effects of spurious light coming back from end bench*, VIR-0246A-06, (2006). 2

[2] B. Canuel, *Diffused light mitigation*, VIR-0679A-08, (2008). 2

[3] B. Canuel, *Diffused light studies*, VIR-0642A-08, (2008). 2

[4] B. Canuel, I. Fiori, J. Marque, E. Tournefier *Diffused light mitigation in Virgo and constraints for Virgo+ and AdV*, VIR-0792A-09, (2009). 2, 3

[5] F. Bondu, *L'interféromètre Virgo : propriétés optiques, stabilisation en fréquence du laser, Mémoire d'habilitation à diriger des recherches.*, June 2008. 3

[6] E. Tournefier, Back-scattering by the optical benches: results from Virgo and constraints for AdV, VIR-0070A-08. 3, 4

[7] John C. Stover, *Optical scattering - measurement and analysis*, SPIE press (1995). 4

[8] I.Fiori, J.Marque, B.Canuel, *End Benches diffused light*, weekly meeting, 30 june 2009, VIR-0321A-09. 9